Biomass Conversion and Biorefinery (2024) 14:11403–11417
https://doi.org/10.1007/s13399-022-03175-9

ORIGINAL ARTICLE

Effect of glycerol addition on the pyrolysis characteristics and pyrolytic product distribution of cigar tobacco

Jian Wu[1] · Zhen Chen[1] · Jun Wang[1] · Yiqun Wang[2] · Jian Jiang[1] · Weiqiang Xiao[1] · Qian Xia[1] · Jiabao Zhang[2] · Guojun Zhou[1] · Junsong Zhang[2] · Miao Liang[2]

Received: 24 May 2022 / Revised: 26 July 2022 / Accepted: 31 July 2022 / Published online: 9 August 2022

Abstract

Cigar tobacco residues are a special air-cured tobacco material with increasing production in domestic. In this present study, the effect of glycerol addition on the pyrolysis characteristic, kinetic behavior, and release of pyrolytic products was investigated by using thermogravimetry coupled with online FTIR and self-built infrared tubular furnace. The thermal weight loss process of cigar tobacco could be divided into four stages, and the glycerol exhibited significant impact on the pyrolysis process. The stage II corresponding the decomposition of volatile components and hemicellulose shifted to the lower temperature accompanied with an increase of DTG_{max} and weight loss at this stage. The T_i, T_f, and residues were decreased, while the CPI was increased as for the CT-G sample, indicating an increased reactivity and comprehensive pyrolysis performance. Gauss peak fitting was used to separate the pyrolysis process of different pseudocomponents in the tobacco biomass. Pyrolysis kinetic analysis based on Coats-Redfern method showed that the activation energy for the decomposition of each pseudocomponents decreased after the addition of glycerol. The online FTIR and MS analysis also reflected the interaction between glycerol and biomass through the release of pyrolytic gaseous products. GC–MS was further used to analyze the compositions of pyrolytic products in the trapped particulate matter under different heating rates. High heating rate was beneficial for the sufficient release of pyrolysis products and aroma compounds. The glycerol addition inhibited the generation of alkaloids, phenols, esters, ketones, acids, and heterocyclic compounds, indicating some effect may exist between cigar tobacco and glycerol.

Keywords Cigar tobacco · Glycerol addition · Pyrolysis characteristics · Thermogravimetric analysis · Aroma compound

✉ Guojun Zhou
zhougj@zjtobacco.com

✉ Miao Liang
liangmiaozzu@163.com

Jian Wu
wujian@zjtobacco.com

Zhen Chen
chenzhen@zjtobacco.com

Jun Wang
wangjun@zjtobacco.com

Yiqun Wang
zzuli505wyq@163.com

Jian Jiang
jiangj@zjtobacco.com

Weiqiang Xiao
xiaowq@zjtobacco.com

Qian Xia
xiaqian@zjtobacco.com

Jiabao Zhang
zzuli505baobao@163.com

Junsong Zhang
13283712413@163.com

[1] Technology Center, China Tobacco Zhejiang Industrial Co., Ltd, Hangzhou 310008, People's Republic of China

[2] Collaborative Innovation Centre of Food Production and Safety, College of Food and Bioengineering, Zhengzhou University of Light Industry, Zhengzhou 450001, People's Republic of China

1 Introduction

Tobacco is a commercial crop widely cultivated worldwide, and China is the largest producer and consumer of tobacco in the world [1, 2]. The tobacco raw materials would experience many complex chemical reactions and physical processes in the burning cigarette product during the suction and smoldering stages [3]. Therefore, the pyrolysis characteristic of tobacco raw materials is an important basis for affecting the release of smoke. From another point of view, large amounts of tobacco residues were produced during the harvest, roasting, and even cigarette manufacturing process [4]. The unreasonable utilization manner of these residual tobacco, such as direct combustion or disposal as waste without treatment, would lead to environmental pollution and waste of bioresources [5, 6]. In fact, the tobacco residues can be converted into energetic and chemical products that usually produced from the fossil fuel, by using the pyrolysis technique [7]. Considering the above two aspects, the study of tobacco pyrolysis is not only beneficial for the formulation design of cigarette product but also for alleviating energy and environmental issues.

Up to now, many efforts have been devoted to the understanding of pyrolysis characteristics or the preparation of energetic products through the thermochemical transformation of different tobacco raw materials, including tobacco leaf fragments, tobacco stem, and tobacco stalk [8–10]. For example, Gao et al. [11] proposed that the pyrolysis process of tobacco stems and leaves included three stages, namely dehydration, main devolatilization, and continuous devolatilization. Sung et al. [12] focused on the non-isothermal pyrolysis behavior of two types of tobacco stem that possessed different chemical compositions using thermogravimetric analyzer. These results showed that the pyrolysis characteristics of tobacco stem was related to the chemical constituents such as the volatile and non-polymeric components. Furthermore, several studies demonstrated that the tobacco waste can be effectively converted into energy products in the forms of biogas, bio-oils, and biochar through pyrolysis process [1]. Liu et al. [13] investigated the pyrolytic properties of tobacco by using pyrolysis–gas chromatography/mass spectrometry (Py-GC/MS), thermogravimetric Fourier transform infrared spectrometry (TG-FTIR), and thermogravimetric mass spectrometry (TG-MS) and pointed out that the components of furfural, aldehydes, ketones, phenols, naphthalenes, indenes, CO, CO_2, etc. constituted the main pyrolytic products. In addition, valuable alkaloidal product nicotyrine can also be selectively produced through the catalytic pyrolysis of tobacco mixed with Pd/C catalyst [14]. Co-pyrolysis of tobacco stalk with different types of polymer wastes also exhibited a synergistic effect compared to the pyrolysis of the individual components, resulting in the change of the distribution and composition of pyrolytic products [15]. Therefore, it can be concluded from the above-mentioned studies that the pyrolysis characteristics and pyrolytic product distribution were greatly influenced by the intrinsic nature of raw materials.

Among the different types of tobacco raw materials, cigar tobacco is an air-cured tobacco material with different physical structure and chemical composition compared to that of flue-cured tobacco leaves [16]. And this difference endows the cigar with unique flavor and aroma characteristic. In recent years, there is a significant growth in domestic cigar tobacco production and consumption along with an inevitable generation of tobacco waste. Meanwhile, research has shown that cigar tobacco is expected to be a potential candidate raw material for the heated tobacco products [17], while the pyrolysis behavior of cigar tobacco was seldom studied, especially the co-pyrolysis with ingredients that usually added during the tobacco processing. Glycerol is an essential ingredient for the processing of tobacco, acting as a moisturizing and surface active agent for flavor application. Previous study has shown that glycerol could exert a certain degree influence on the composition content of released mainstream gas during the pyrolysis of tobacco [18]. Gómez-Siurana et al. [19] studied the pyrolysis behavior of glycerol-tobacco (flue-cured tobacco) mixture by TG-FTIR and proposed that possible interaction between glycerol and tobacco were existed. In addition, the presence of glycerol seems to change the pathway of the generation of pyrolytic gases. Therefore, it is necessary to further understand the effect of glycerol addition on the pyrolysis behavior of cigar tobacco, which would facilitate the reasonable utilization of cigar tobacco leaves or the corresponding waste.

However, the effect of glycerol on the pyrolysis characteristics and pyrolytic product distribution of cigar tobacco are not well interpreted. Herein, an in-depth study on the pyrolysis behavior of cigar tobacco with or without glycerol addition was conducted. The reaction kinetics and volatile gas release behavior during the pyrolysis process were investigated by using TG-FTIR/TG-MS and Coats-Redfern method. Furthermore, the cigar tobacco and tobacco-glycerol mixture were pyrolyzed in an infrared-heated fixed bed reactor under different heating rates, and the pyrolytic smoke components were captured by Cambridge filter and determined by GC–MS. This study may be beneficial to the rational utilization of cigar tobacco waste through the thermochemical conversion route.

2 Materials and methods

2.1 Materials

The naturally fermented upper cigar tobacco leaves were collected from Dongfang city, Hainan Province of China. The variety of the cigar tobacco was Yongsheng No. 3.

High purity of glycerol (AR, 99%), ethanol (GR, ≥ 99.5%), dichloromethane (99%), and phenylethyl acetate (GR, ≥ 99.5%) were purchased from Aladdin Chemical Reagent Inc. of Shanghai, China.

The cigar tobacco with glycerol addition was prepared as follows. The original tobacco sample was dried in oven at 120 °C for 5 min to remove the excessive water. Then, the dried cigar tobacco leaves were mixed with ethanol-diluted glycerol, and the added glycerol content was 15 wt% of the cigar leaves. After that, the tobacco-glycerol mixtures were sealed in a ziplock bag for the adequate absorption of the glycerol. The detected amount of glycerol by gas chromatographic method (Chinese Specification YC/T 243–2008) was 13.49 wt% after the storage, which was basically consisted with that of theoretical addition amount. Subsequently, the samples were equilibrated overnight in a constant temperature and humidity chamber that set at 22 °C and 40% RH. Then, the sample was crushed through a multifunctional disintegrator (DSY500A, Zhuokai Electrical Appliance, China) and sieved to obtain the powdered (60 mesh) feedstock for further analysis. The original cigar tobacco and tobacco-glycerol mixtures were denoted as CT and CT-G, respectively.

2.2 Pyrolysis characteristic analysis

The pyrolysis characteristics of CT and CT-G samples were analyzed through the thermal weight loss process using thermogravimetric analyzer (TGA, Q5000, USA). Approximately 10 mg of sample was loaded into the platinum crucible and heated from 40 to 800 °C under the heating rate of 30 °C/min. The carrier gas was nitrogen with a flow rate of 40 mL/min. The pyrolysis characteristic parameters, including the initial and final pyrolysis temperature (T_i and T_f), the maximum pyrolysis rate (DTG_{max}), and its corresponding temperature (T_{max}), were determined from the TG and derivative thermogravimetry (DTG, first-order derivative of TG curve) profiles. Then, the comprehensive pyrolysis index (CPI) of CT and CT-G can be calculated from the following formula [20]:

$$\mathrm{CPI} = \frac{DTG_{max}}{T_{max} \times (T_f - T_i)} \tag{1}$$

The released gaseous products during the pyrolysis process were monitored through an online FTIR spectrometer (Nicolet 8700, Thermo Electron, America) that connected to the thermogravimetric analyzer, in the wavenumber range of 400 to 4000 cm^{-1} at a resolution of 2 cm^{-1}. The transfer line for the transportation of gaseous products between the TG and FTIR was heated to 230 °C to avoid the condensation of pyrolytic gas. Meanwhile, pyrolysis of the samples was also carried out using a TG-MS analyzer (Thermo Mass Photo, Japan). Helium at a flow rate of 150 mL/min was selected as carrier gas. The identification of some typical gaseous products was obtained from the mass spectrometer by monitoring evolved MS fragments as a function of temperature.

In addition, the interaction between glycerol and cigar tobacco was compared by using the theoretical TG versus the experimental curves. The theoretical value and the deviation (%) that used to assess the interaction degree between individual components were calculated according to Eq. (2) and Eq. (3), respectively [21].

$$Y_{theo} = x_1 Y_1 + x_2 Y_2 \tag{2}$$

$$\mathrm{Deviation}(\%) = \left(\frac{Y_{theo} - Y_{exp}}{Y_{exp}}\right) \times 100 \tag{3}$$

where *Y1*, *Y2* are the corresponding mass loss and *x* is the mass ratio of each component.

2.3 Pyrolysis kinetic analysis

The pyrolysis of tobacco is a complex inhomogenous reaction accompanied by the consecutive and overlapping thermal decomposition processes of four main components (volatile components, hemicellulose, cellulose, and lignin) in the feedstock, thus resulting in an informative TG and DTG curves. Multi-peak fitting method can effectively separate overlapping subpeaks in complex curves. Then, Gauss peak fitting module of OriginPro software was used to separate the four components' reaction rate curves from the DTG curves of CT and CT-G. The proportions of the four components of the samples were then adopted for the pyrolysis kinetic analysis to investigate the effect of glycerol addition.

Generally, for the pyrolysis reaction of complex biomass, a pseudocomponents parallel reaction model can be used to describe the thermal decomposition process [22]. And the total pyrolysis reaction rate equation can be regarded as the weighted sum of each pseudocomponent. The thermal reaction rate equation of each pseudocomponent was described by the following formula [23]:

$$\frac{\mathrm{d}\alpha_i}{\mathrm{d}T} = k_i(T) f_i(\alpha_i) \tag{4}$$

where the subscript *i* represents the four components, that is volatile components, hemicellulose, cellulose, and lignin of the tobacco sample. α_i is the thermal conversion fraction of the corresponding component at temperature *T*, which can be calculated by integrating the DTG curve of component *i* after the split peak fitting; $f_i(\alpha_i)$ is a general expression of the reaction model of component *i* that expressed as function

of α_i; and $k_i(T)$ is the reaction rate constant of component i, which is given by Arrhenius equation:

$$k_i(T) = A_i \exp(-\frac{E_i}{RT}) \tag{5}$$

where A_i and E_i are the pre-exponential factor (1/min) and activation energy (kJ/mol) of component i during its pyrolysis reaction, respectively; R is the universal gas constant of 8.314 J/K mol; and T is the absolute temperature (K).

Then, a combined and rearranged form of Eqs. (4) and (5) is transformed into

$$\frac{d\alpha_i}{dT} = \frac{A_i}{\beta}\exp\left(-\frac{E_i}{RT}\right) f_i(\alpha_i) \tag{6}$$

The kinetic parameters can be obtained from the nonisothermal TGA data through the above Eq. (6). By separation of variables and integration of Eq. (6), it can be expressed as [24]

$$G_i(\alpha_i) = \int_0^{\alpha_i} \frac{d\alpha_i}{f_i(\alpha_i)} = \int_{T_0}^{T} \frac{A_i}{\beta}\exp(-\frac{E_i}{RT})dT \tag{7}$$

where $G_i(\alpha_i)$ is the integral function of reaction model $f_i(\alpha_i)$. Many approximation methods have been developed to solve the above equation.

In this study, Coats-Redfern approximation method was adopted to calculate the kinetic parameters of non-isothermal pyrolysis of tobacco, and Eq. (7) can be transformed into the following logarithmic form [25]:

$$\ln\left[\frac{G_i(\alpha_i)}{T^2}\right] = \ln\left[\frac{A_i R}{\beta E_i}(1 - \frac{2RT}{E_i})\right] - \frac{E_i}{RT} \tag{8}$$

As for the value of $2RT/E_i$ is close to zero, the above equation can be simplified as follows:

$$\ln\left[\frac{G_i(\alpha_i)}{T^2}\right] = \ln\frac{A_i R}{\beta E_i} - \frac{E_i}{RT} \tag{9}$$

Activation energy E_i and pre-exponential factor A_i of component i during the pyrolysis process can be calculated from the slope and intercept of the linear fitting of $\ln [G_i(\alpha_i)/T^2]$ against 1/T, respectively.

Furthermore, the thermochemical parameters for each component including enthalpies (ΔH), Gibbs free energies (ΔG), and entropies (ΔS) can also be calculated by the following Eqs. [8, 26]:

$$\Delta H = E_i - RT_{maxi} \tag{10}$$

$$\Delta G = E_i + RT_{maxi}\ln\left(\frac{K_B T_{maxi}}{hA_i}\right) \tag{11}$$

$$\Delta S = \frac{\Delta H - \Delta G}{T_{maxi}} \tag{12}$$

where K_B is the Boltzmann constant (1.381×10^{-23} J/K) and h is the Planck constant (6.626×10^{-34} J·s).

2.4 Pyrolysis experiment and pyrolytic product analysis

The pyrolysis experiment of tobacco samples was further conducted on an infrared heated tubular furnace depicted in Fig. 1. The reactor was continuously flushed with nitrogen under a flow rate of 300 mL/min to ensure an inert atmosphere and reduce the residence time and secondary reactions of vapors. In a typical experiment, the tobacco sample with a weight of 1.0 g was firstly loaded into a quartz boat and placed into the infrared heating zone. Then the sample was heated to 750 °C and

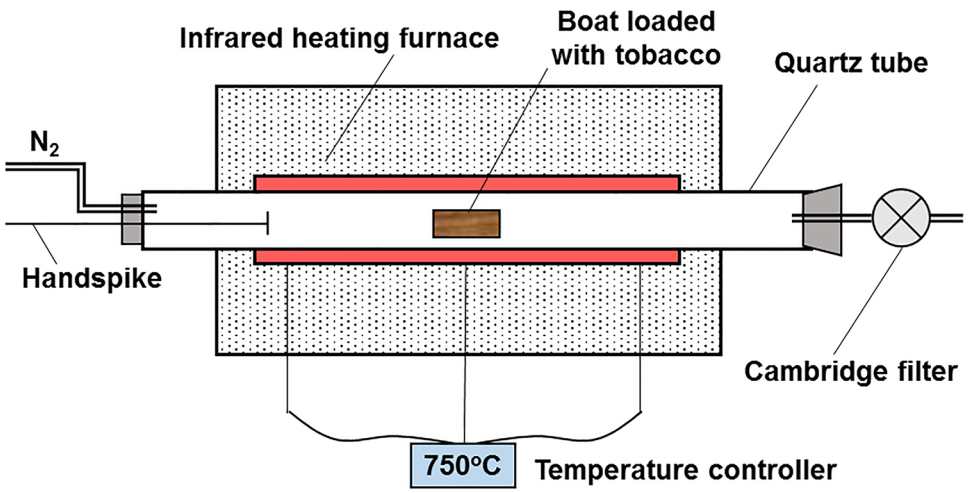

Fig. 1 Schematic diagram of the pyrolysis reactor

maintained at this temperature for a specific time under a heating rate of 30 °C/min or 250 °C/min, which denoted as slow pyrolysis and fast pyrolysis, respectively. The pyrolytic smoke passed through the Cambridge filter held by the holder and was trapped by the filter. The trapped pyrolysis products of CT and CT-G under slow and fast heating rate were denoted as CT-S, CT-F, CT-G-S, and CT-G-F, respectively. Meanwhile, the pyrolytic char under different conditions was collected for the elemental compositions and chemical group analysis. An elemental analyzer (Vario EL cube; CHNS, Germany) was used to analyze the organic element contents of the samples. The oxygen element content of the sample was calculated by difference. FTIR analysis was conducted using a Nicolet 6700 FTIR spectrometer (Thermo Scientific, USA) in the range of 400–4000 cm^{-1} with pure KBr pellet as background.

The pyrolytic products in the particulate matter that collected by the filter were then extracted by dichloromethane, concentrated, and analyzed by using a 8890-5977B GC–MS analyzer (Agilent, USA) coupled with a HP-5 capillary column (60 m long, 0.25 mm diameter with a film thickness of 0.25 μm). The carrier gas was high-purity helium, and its flow rate was set at 1.0 mL/min. The temperature program of column oven was set as follows: at a constant temperature of 40 °C for 5 min, 40–250 °C at a rate of 3 °C/min, followed by 250–280 °C at a rate of 20 °C/min, and remained at this temperature for 5 min. The mass spectrometer was operated under the electron impact (EI) mode with electron energy at 70 eV and scanning range of 35–550 m/z in the full scan mode method. The quadrupole temperature, ion source temperature, and the transfer line temperature were 150 °C, 230 °C, and 280 °C, respectively. The extracted sample was firstly passed through a 0.45 μm nylon microfilter prior to the analysis to remove impurities and mixed with a specific concentration of phenylethyl acetate-dichloromethane compounds used as internal standard for quantification. The products were identified by matching against the NIST database.

3 Results and discussion

3.1 TG analysis of CT and CT-G

The pyrolysis behavior of CT and CT-G samples were analyzed through TG technique, and the weight loss curves and corresponding DTG profiles were presented in Fig. 2. The thermal weight loss process of both samples can be divided into four stages from the temperature intervals in DTG curves, which were corresponded to the dehydration (stage I), decomposition of volatile components and hemicellulose (stage II), decomposition of cellulose and lignin (stage III), and decomposition of inorganic salts (stage IV), respectively. Actually, the decomposition stage of different types of tobacco have already been described and assigned in previous studies, while the decomposition process of CT sample in this study was somewhat different from that of the reported flue-cured tobacco which usually exhibited an obvious DTG peak at around 200 °C due to the volatilization and decomposition of volatile non-polymeric tobacco constituents [3, 8, 12].

Moreover, it can be observed that there existed some differences in the thermal decomposition curves between the CT and CT-G sample. The temperature intervals and weight loss proportion at different decomposition stages were summarized in Table 1. Meanwhile, Table 2 presents the pyrolysis characteristic parameters such as the T_{max} and DTG_{max}. The temperature interval for the release of moisture in CT sample was 30–143 °C with a maximum temperature at 89 °C. As for the CT-G sample, the temperature intervals shifted to the lower temperature and only exhibited a slowdown dehydration process. The weight loss at this stage was increased from 5.81% to 7.67% after the introduction of glycerol into the tobacco due to its humectant effect. The temperature interval for stage II was 143–295 °C with a weight loss of 23.52% for CT sample. Actually, two overlapped decomposition processes occurred in this stage, which were assigned to the volatilization of low-boiling organic compounds (such as soluble sugars, pectin, and nicotine) and the decomposition of hemicellulose [12, 19]. The

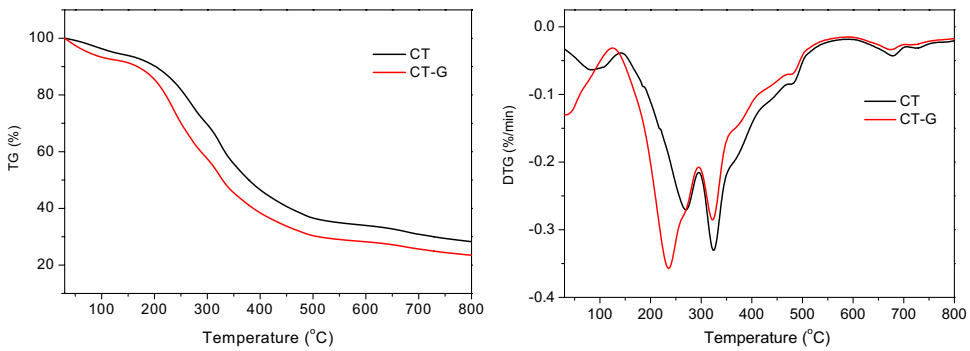

Fig. 2 TG and DTG curves of CT and CT-G samples under N_2 atmosphere

Table 1 Weight loss at different decomposition stages during pyrolysis of CT and CT-G

Decomposition stage	CT		CT-G	
	Temperature intervals (°C)	Weight loss (%)	Temperature intervals (°C)	Weight loss (%)
Stage I	30–143	5.81	30–126	7.67
Stage II	143–295	23.52	126–295	33.83
Stage III	295–586	36.43	295–586	30.07
Stage IV	586–800	5.98	586–800	4.96

Table 2 Pyrolysis characteristic parameters of CT and CT-G during the pyrolysis process

Sample	T_i (°C)	T_{max} (°C)		DTG_{max} (%/min)		T_f (°C)	CPI (10^{-6}%/(min × °C^2))	Residues (%)
		Stage II	Stage III	Stage II	Stage III			
CT	213.1	269.3	324.3	0.27	0.33	402.1	5.38	28.26
CT-G	198.0	235.5	322.8	0.36	0.28	392.5	5.73	23.47

peak temperature of 269.3 °C at this stage was originated from the thermal decomposition of hemicellulose which was the major components of tobacco leaves and stem. And previous study on the hemicellulose pyrolysis has also found the major weight loss for hemicellulose occurred between 220 and 315 °C with a maximum rate at around 260 °C [27]. While as compared with that of flue-cured tobacco [8, 11], the weight-loss peak for the volatile components was overlapped and almost absent may be due to the low content of these compounds in CT. After the addition of glycerol, the temperature interval of stage II was ranged from 126 to 295 °C with an increased weight loss of 33.83%. The T_{max} of this stage was shifted to 235.5 °C which can be attributed to the volatilization of glycerol and other endogenous volatile components [28]. At the same time, a small shoulder peak at around 260 °C that originated from the decomposition of hemicellulose can also be observed. The decreased T_{max} and increased DTG_{max} in stage II may indicate that some interaction between CT and glycerol could occur, and the addition of glycerol promoted the volatilization and release of pyrolytic compounds.

The temperature interval of stage III for both CT and CT-G was also between 295 and 586 °C with the peak temperature at 324.3 °C and 322.8 °C, respectively. The DTG peak at this stage was corresponded to the decomposition of cellulose, and the DTG_{max} was decreased from 0.33 to 0.28%/min after the addition of glycerol. Moreover, the decomposition of lignin and subsequent carbonization reactions also occurred at this stage accompanied by two faint and diffuse peaks at higher temperatures, which may be related to the small amount and wide pyrolysis temperature range of lignin in the CT samples [11]. A decreased weight loss from 36.43 to 30.07% was observed at stage III, which may be related to the dissolution of lignin due to the formed hydrogen bonds between alcoholic hydroxyl and the free hydroxyl of lignin during the pretreatment and heating process of CT-G [29]. The temperature interval at 586–800 °C was corresponded to the dehydrogenation and aromatization of char and decomposition of inorganic salts. The weight losses of CT and CT-G at stage IV were 5.98% and 4.96%, respectively.

The pyrolysis characteristic parameters, such as T_i, T_f, and CPI, were calculated and listed in Table 2. The addition of glycerol significantly decreased the T_i and T_f, indicating an increased reactivity due to the introduction of exogenous volatile component. The char residues after the pyrolysis process decreased from 28.26 to 23.47% after the addition of glycerol, indicating the promoting effect of glycerol on the release of pyrolytic gaseous products and the inhibiting effect on the char formation in the pyrolysis process of tobacco. And this similar effect of glycerol on the pyrolysis of flue-cured tobacco was also found in previous study of Dai et al. [3]. In addition, the CPI was calculated to quantitatively evaluate the pyrolysis characteristic of tobacco samples. As can be seen, the CPI was increased from 5.38×10^{-6}%/(min × °C^2) to 5.73×10^{-6}%/(min × °C^2) after the addition of glycerol, indicating a positive effect of glycerol on the pyrolysis reactivity by changing the chemical composition of CT.

The deviation of weight loss during the co-pyrolysis process of glycerol and CT was shown in Fig. 3. As can be seen, the deviation between the theoretical and experimental TG curves was positive in the whole pyrolysis temperature range, indicating a promoting interaction happened between glycerol and CT [4]. Two maximum peaks at 234.0 °C and 334.5 °C were exhibited, which corresponded to the T_{max} of Stages II and III, respectively. The reason for this phenomenon can be ascribed to the thermal effect of glycerol promoting the release and decomposition of intrinsic substance. In addition, the porous structure of biochar produced from CT-G may also contribute to the heat and mass transfer, while the promoting interaction all along with the pyrolysis

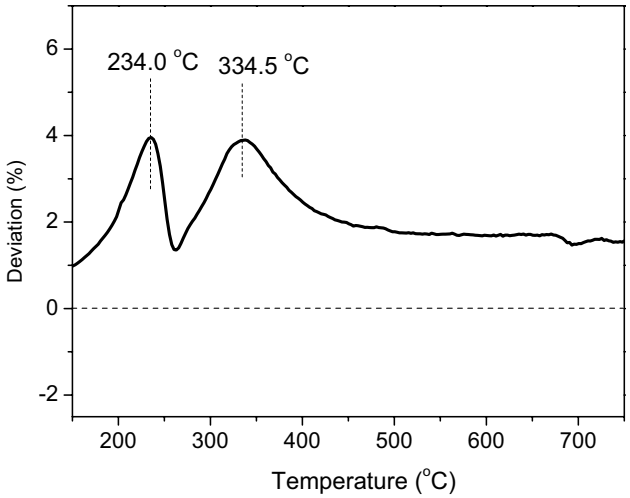

Fig. 3 Deviation of TG due to co-pyrolysis of glycerol and CT

temperature herein was different from the co-pyrolysis process of other biomass, such as the co-pyrolysis of sewage sludge and rice husk or the reclaimed asphalt and wood sawdust [21, 30].

3.2 Gauss peak fitting and pyrolysis kinetic analysis

The pyrolysis of tobacco contains many complex parallel and serial chemical reaction processes due to the multicomponent compositions and different reactivity, resulting in the cross-overlap of DTG peaks. The above described different superimposed DTG peaks are usually caused by the different components and their pyrolysis characteristics during the reaction process. In order to further understand the pyrolysis behavior of different components in tobacco, a Gauss peak fitting method was used to separate the main weight loss processes on the DTG profile. As shown in Fig. 4, five pyrolysis processes were obtained by peak splitting, which could be sequentially assigned to the decomposition of volatile components, hemicellulose, cellulose, lignin, and carbonization process according to previous studies [31, 32]. The peak temperature center and percent areas under each separated peak were listed in Table 3. The area of peak 1 increased from 10.9 to 19.4% due to the introduction of glycerol which usually exhibited a maximum DTG-peak at around 219 °C [19]. The decomposition temperatures for hemicellulose and cellulose were reported at 225–325 °C and 325–375 °C, respectively [31], and the temperature ranges of separated peak 2 and 3 were basically in accordance with the previous data. Meanwhile, it can be found that the center temperature of peak 2 decreased to 253.7 °C accompanied with an increase in the peak area, which may indicate a positive effect of glycerol on the decomposition and release of the reactants in this region, while the added glycerol exhibited relative small effect on the decomposition of cellulose. As for the peak 4 and 5, it was reported that the lignin presented a gradual degradation and carbonization process over a relative wide temperature range of 250–500 °C. The addition of glycerol decreased the peak areas at this two stages, which

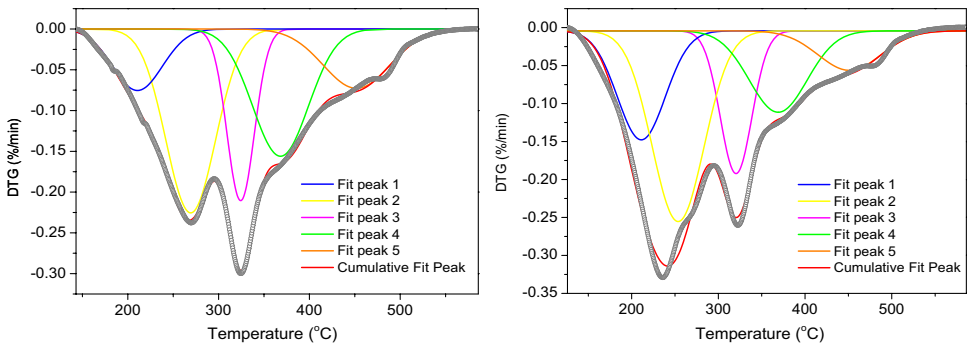

Fig. 4 Gauss peak fitting of the main weight loss processes for CT and CT-G samples

Table 3 Temperature peak and percent areas under curve of each separated peak

Peak number	CT		CT-G	
	Peak center	Percent area (%)	Peak center	Percent area (%)
Peak 1 (Volatile components)	210.7	10.9	211.2	19.4
Peak 2 (Hemicellulose)	269.3	32.6	253.7	36.9
Peak 3 (Cellulose)	324.3	16.9	320.5	16.8
Peak 4 (Lignin)	368.2	25.4	369.0	17.5
Peak 5 (Carbonization)	452.0	14.2	451.3	9.3

may be related to the dissolution effect of glycerol on lignin as stated above.

The pyrolysis kinetic behavior of each separated Gauss peak was studied through the calculation method described in Sect. 2.3. The optimum reaction model for describing the pyrolysis of different components was considered as F1.5 reaction model according to the fitting results as shown in Fig. 5. The calculated kinetic parameters for the pyrolysis of each pseudocomponent were listed in Table 4. As both for the CT and CT-G samples, the decomposition of volatile components (Peak 1) and cellulose (Peak 3) exhibited the lowest and highest E_i values, respectively. The E_i for lignin decomposition was higher than that of hemicellulose and lower than that of cellulose. In addition, compared to the activation energies of flue-cured tobacco ranging from 50 to 150 kJ/mol, the E_i here was relatively high and was basically the same as the activation energies of tobacco stem [7, 8]. In another word, the pyrolysis reaction of CT might be more difficult to react, and thus appropriate pretreatment or additives are necessary during the conversion of CT into valuable products. After the addition of glycerol, the E_i for each pseudocomponent was decreased to varying degrees in the range of 13.5–28.4%, especially for the decomposition of cellulose and hemicellulose process. This result may indicate that glycerol reduced the reaction barriers for the decomposition of tobacco components and promoted the degradation or release of pyrolytic products. This phenomenon can be ascribed from the changed composition and microstructure during the pyrolysis process of biomass.

Moreover, the thermodynamic parameters including ΔH, ΔG, and ΔS were also calculated according to the formulas (10)–(12) and presented in Table 4. The variation of ΔH for both CT and CT-G was consistent with that of corresponded Ei values. Generally, the ΔH reflects the total energy consumed for the thermal conversion of biomass into various pyrolytic products. Additionally, the decreased ΔH of CT-G for different pyrolysis processes under the separated peaks indicated a less energy required to break the chemical bonds of CT-G. ΔG is usually considered to reflect the total energy increase of the reaction system at the approach of the

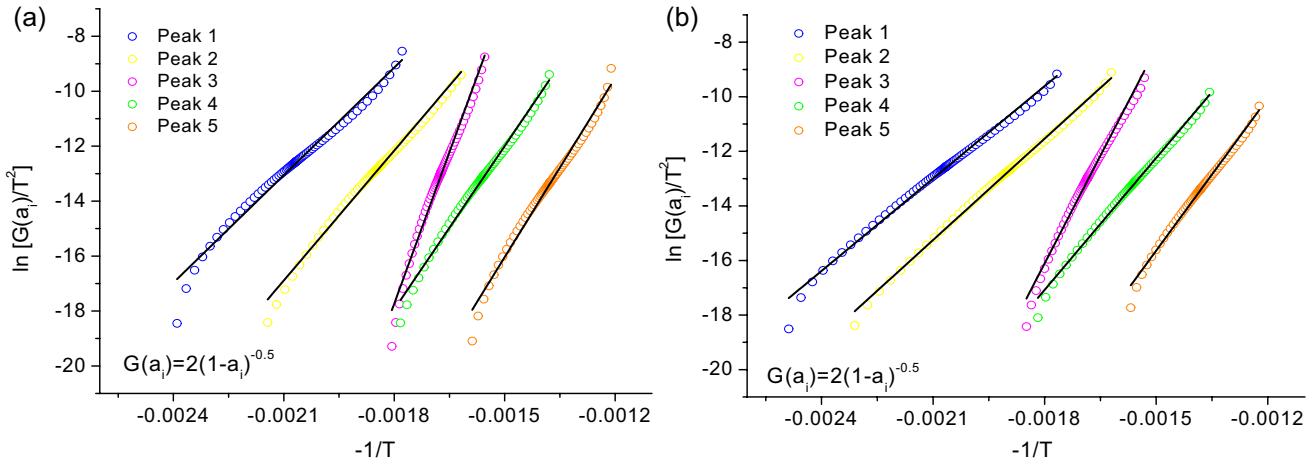

Fig. 5 Fitting of F1.5 reaction model of the separated thermal decomposition stages of CT (**a**) and CT-G (**b**) samples based on the Coats-Redfern method

Table 4 Pyrolysis characteristic parameters of CT and CT-G during the pyrolysis process

Sample	Peak number	Reaction model	Fitted equation	R^2	Ei (kJ/mol)	Ai (min^{-1})	ΔH (kJ/mol)	ΔG (kJ/mol)	ΔS (kJ/mol)
CT	Peak 1	F1.5	y = − 13,049.44x + 14.35	0.978	108.49	6.68×10^{11}	104.47	135.88	− 0.065
	Peak 2	F1.5	y = − 15,760.00x + 16.21	0.990	131.03	5.18×10^{12}	126.52	153.02	− 0.049
	Peak 3	F1.5	y = − 36,764.14x + 48.45	0.981	305.66	1.21×10^{27}	300.69	166.02	0.23
	Peak 4	F1.5	y = − 19,807.86x + 17.72	0.991	164.68	2.94×10^{13}	159.35	182.32	− 0.036
	Peak 5	F1.5	y = − 21,719.23x + 16.54	0.985	180.57	9.96×10^{12}	174.54	207.77	− 0.046
CT-G	Peak 1	F1.5	y = − 11,292.10x + 10.72	0.991	93.88	1.53×10^{10}	89.50	140.63	− 0.097
	Peak 2	F1.5	y = − 12,387.83x + 10.76	0.997	102.99	1.76×10^{10}	98.48	150.62	− 0.096
	Peak 3	F1.5	y = − 26,312.69x + 31.26	0.986	218.76	2.96×10^{19}	213.82	166.47	0.080
	Peak 4	F1.5	y = − 16,117.56x + 11.93	0.994	134.00	7.37×10^{10}	128.66	183.63	− 0.086
	Peak 5	F1.5	y = − 18,605.82x + 12.27	0.990	154.69	1.19×10^{11}	148.67	208.52	− 0.083

reagents and the formation of activated complex [33], and the value of Δ*G* increased with the elevation of the depth of the pyrolysis process. This phenomenon indicated that the difficulty in the occurrence of pyrolysis reactions increased with the deepening of the pyrolysis process. Meanwhile, the Δ*G* values of CT-G were slightly higher than that of CT under different Gauss fitted peaks except for the pyrolysis of hemicellulose. The Δ*S* reveals the deviation degree of the system from its own thermodynamic equilibrium state. The fluctuation of the Δ*S* values reflected the reactivity of the different pseudocomponent was unstable during the pyrolysis process. In particular, as for the CT-G sample, the increase in absolute values of Δ*S* for the formation of activated complex indicated the reactants was far from the thermodynamic equilibrium, and thus the reactivity of materials was high to form the activated complex [26]. The thermodynamic parameters here may indicate that the reaction reactivity of CT-G was promoted as compared with the CT sample.

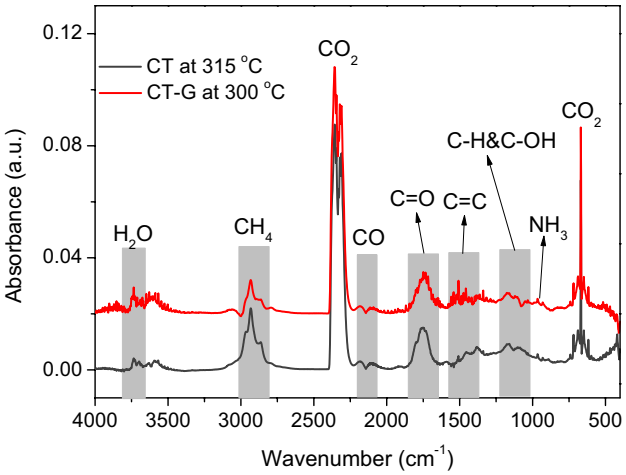

Fig. 7 FTIR spectrum of the released gaseous products around the T_{max} of stage III

3.3 Online analysis of pyrolytic gaseous products by TG-FTIR and TG-MS

The online FTIR technique was connected to the TG equipment to monitor the released gaseous products during the pyrolysis process. The three-dimensional FTIR spectrum of the pyrolytic gaseous products from CT and CT-G was shown in Fig. 6. The evolution of absorbance peaks with time was basically consistent with the weight loss process in the DTG profiles, and some difference in the released gaseous products can be observed from Fig. 6. Figure 7 presents the spectra of pyrolytic products at around the DTG peak for the decomposition of cellulose stage, and the functional groups corresponded to different wavenumber were assigned according to the literature [34]. Permanent gaseous products including H_2O, CH_4, CO_2, and CO can be readily identified through their characteristic absorbance bands. The appearance of distinctive absorption band at 1860–1640 cm^{-1} represented the stretching vibration of C = O, indicating the generation of ketone, aldehyde, and acids during the pyrolysis of tobacco. The absorption band between 1570 and 1350 cm^{-1} was corresponded to the vibration of C = C stretching and benzene skeleton, which indicated the presence of aromatics in the pyrolysis of biomass [35]. The small absorption band located at around 1160 cm^{-1} can be attributed to the C–OH stretching vibration of alcohols and phenols. The presence of NH_3 can be identified through the band at 952 cm^{-1} according to the study of Kruse et al. [36]. And the bands for other nitrogenous compounds may be overlapped by the bands corresponding to other compounds in the low wavenumber zone.

The evolution of absorbance intensity of typical functional groups with temperature during the pyrolysis of

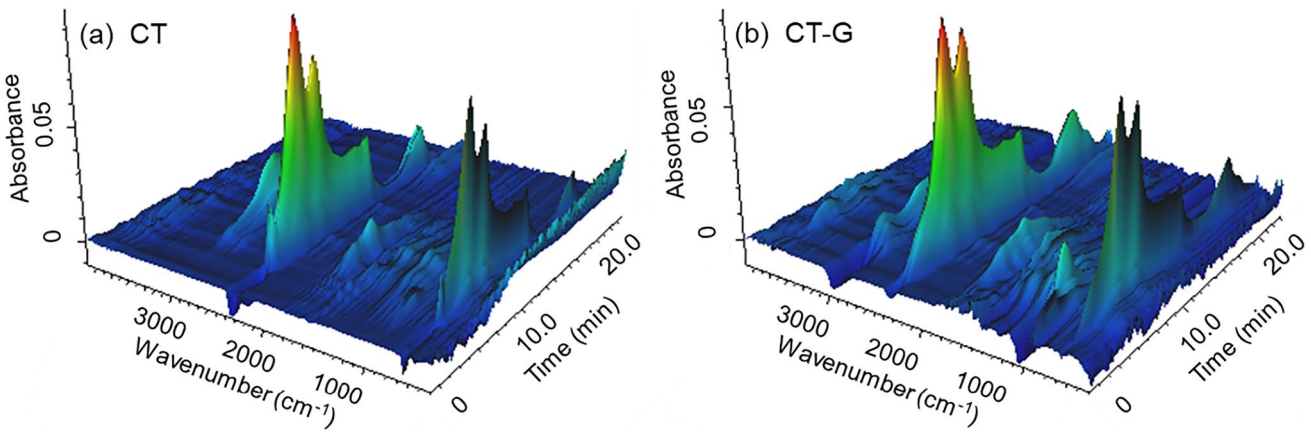

Fig. 6 Three-dimensional FTIR spectrum of gaseous products from the pyrolysis of CT (**a**) and CT-G (**b**)

CT and CT-G was compared in Fig. 8, in order to further evaluate the influence of glycerol. The main release temperature interval of H_2O corresponded to the decomposition of hemicellulose and cellulose stages through the cleavage of hydroxyl groups in these biopolymer. The overall higher absorbance intensity of CT-G sample may reflect some interaction between glycerol and tobacco. As for the other selected pyrolytic products, glycerol may decrease the maximum release temperature and the absorbance intensity. CH_4 and aromatics that formed mainly through the decomposition of lignin exhibited two-stage release characteristics for CT-G, indicating the significant effect between glycerol and lignin. The main gaseous phase product CO_2 can be generated from

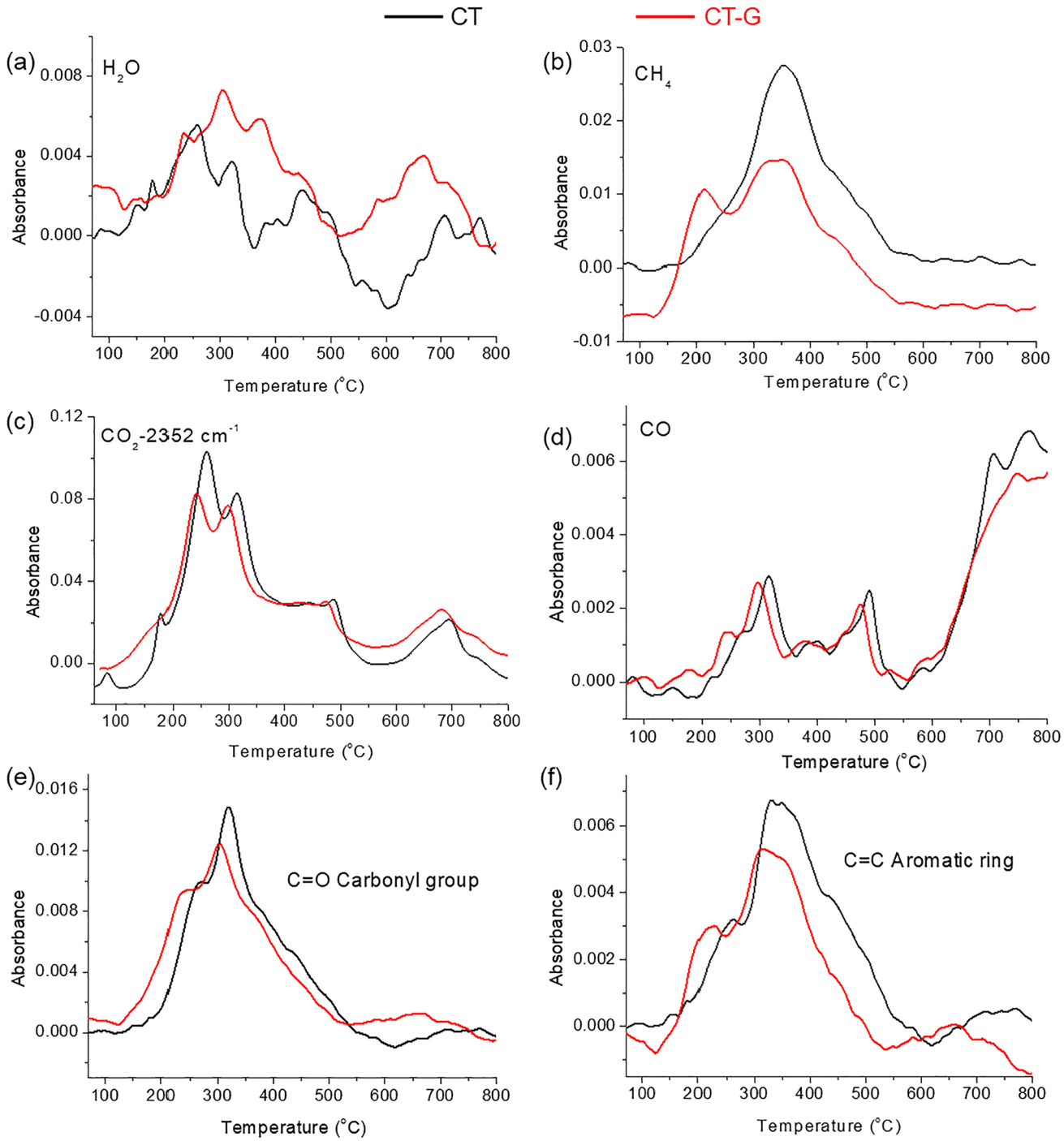

Fig. 8 FTIR spectrum of the released gaseous products around the T_{max} of stage III

the cracking reaction of oxygen-containing compounds at below 550 °C and the further decarboxylation reaction during the carbonization process at around 700 °C [37]. A slight increase of CO_2 was observed at temperature higher than 550 °C after the addition of glycerol, which was consistent with the study of Gómez-Siurana et al. [19]. In addition, the production of CO and carbonyl groups was also affected by the introduction of glycerol. These observations of the released gaseous products indicated that the glycerol not only affected the pyrolysis characteristic but also the pyrolytic product distribution.

Furthermore, the releasing profile of characteristic MS fragments during the pyrolysis process were recorded by using TG-MS. Figure 9 presents the six mass fragments of m/z = 79, 84, 95, and 107 that can be assigned to pyridine, nicotine, $C_5H_3O_2^+$, and $C_7H_7O^+$, respectively [38, 39]. Pyridine was the main pyrolytic products of air-cured tobacco, which can be produced from the pyrolysis process of nitrogenous compound. The two-stage releasing profile of pyridine fused into one peak centered at around 526 °C after the addition of glycerol. Nicotine was the typical component in the pyrolytic products of tobacco, which exhibited a two-stage release characteristic. This phenomenon may be related to the speciation and occurrence state of nicotine in the tobacco. And the presence of glycerol may change the thermal stability of nicotine under high temperature. The $C_5H_3O_2^+$ mainly arose from furfural that was an important pyrolytic product of polysaccharide [40]. The release of $C_5H_3O_2^+$ occurred not only in the hemicellulose and cellulose decomposition stage, but also in the pyrolysis stage of lignin. The $C_7H_7O^+$ can be ascribed to phenols containing methyl and methoxy groups, which were mainly produced from the decomposition of lignin. The introduction of glycerol increased the release amount of $C_7H_7O^+$ in lower temperature, while shifted the maximum release peak to higher temperature and reduced the corresponding release amount. In addition, it can be seen from the cumulative release of these characteristic mass fragments that the addition of glycerol decreased the release amount of products during the pyrolysis of unit mass samples.

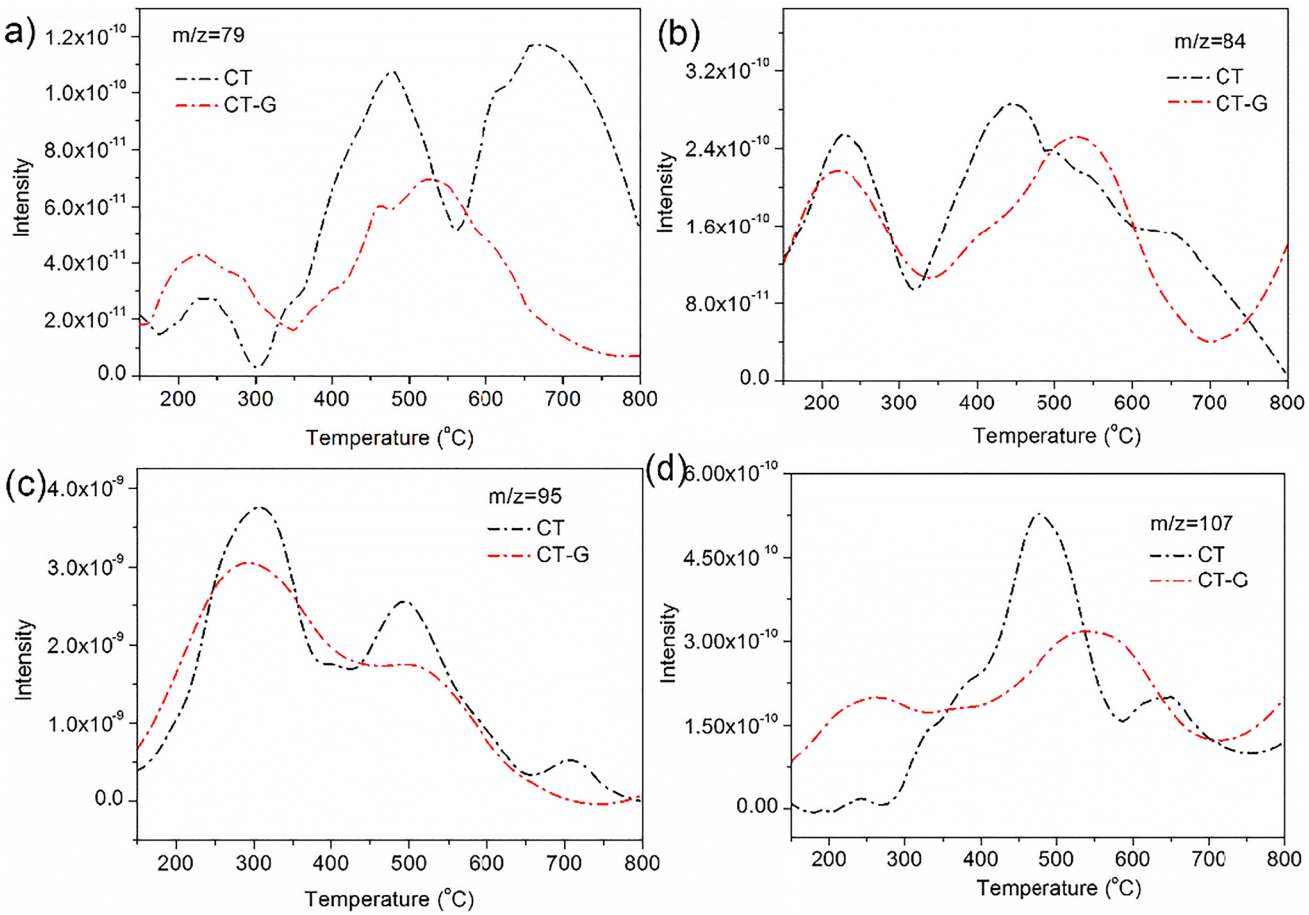

Fig. 9 Evolution of the characteristic MS fragments of **a** pyridine, **b** nicotine, **c** furfural, and **d** phenols during the pyrolysis process of CT and CT-G

3.4 GC–MS analysis of trapped particulate matters

The pyrolytic products under slow and fast heating rates that trapped by the Cambridge filter were further analyzed through GC–MS. First of all, the filter was weighted before and after capturing the particulate matters, and it was found that the addition of glycerol increased the release of pyrolytic smoke from CT. Fast heating rate also enhanced the weight of pyrolytic particulate matters significantly. Meanwhile, the composition and content of each pyrolytic product were determined and summarized in Table S1. The pyrolytic products can be classified into alkaloids, heterocyclic, olefins, phenols, ketones, alcohols, acids, esters, amines, aldehydes, and other compounds. The contents of compounds in different classifications for samples of CT-S, CT-G-S, CT-F, and CT-G-F were calculated and shown in Table S2 and Fig. 10. In addition, we also collected the pyrolytic chars produced under different conditions and analyzed the elemental compositions and chemical groups, and the results were shown in Table S3 and Figure S1. It seemed that the chars generated under slow heating rate possessed higher content of C element, and the content of N, H and S element exhibited little difference between chars. FTIR analysis showed the characteristic bands related to the vibration of functional groups of –OH, $-CH_2/-CH_3$, C = C, and C-O.

It can be seen from Table S1 that the main pyrolytic products trapped by Cambridge filter for CT samples included nicotine and other alkaloids, 2-furanmethanol, phenols, 2-pyrrolidinone, pyridinol, neophytadiene, etc. The heating rate exhibited an important influence on the distribution of pyrolysis products. As can be seen from Fig. 10 that the fast heating rate was favorable for the release of pyrolysis products and aroma compounds. For instance, the contents of various classification of compounds were increased to some extent except for the esters and alkanes, especially for the alkaloids, heterocyclic, ketones, and aldehyde compounds. Some ketones compounds that usually exhibited special aroma characteristics, such as 2-cyclopenten-1-one, 2-methyl-2-cyclopenten-1-one, 5-methyl-2(5H)-furanone, and 2,3-dimethyl-2-cyclopenten-1-one, were only produced under fast heating rate. Heterocyclic compounds, such as pyridine and pyrroles, that produced from the pyrolysis of nitrogen-containing precursor in CT were also preferred to generate under high heating rate. In addition, the introduction of glycerol could slightly inhibit the generation of alkaloids, phenols, esters, ketones, acids, and heterocyclic compounds, which was basically consistent with the above online FTIR and MS analysis. For example, phytol and palmitic acid reduced to 105.96 μg/g and 160.07 μg/g, respectively, under fast heating rate. Phenol compounds usually produced from the decomposition of lignin and the secondary products [41]. The decreased release of phenols such as phenol, p-cresol, and 4-ethyl-phenol may relate to the effect between glycerol and lignin. Large amount of glycerol were detected in the pyrolytic products of CT-G samples, that is 1057.87 μg/g and 1226.86 μg/g under the slow and fast heating rate, respectively. The detected glycerol was ascribed to the direct evaporation and transfer of glycerol at low temperature pyrolysis interval. An important tobacco flavor precursor, thunbergol (162.27 μg/g), was determined only after the addition of glycerol under fast heating rate. In addition, the contents of some aroma compounds that contributed to the aroma style of tobacco were released or increased under fast heating rate, such as acetoin, 2-cyclopenten-1-one, 3-methyl-2-cyclopenten-1-one, 2,3-dimethyl-2- cyclopenten-1-one, 3-methyl-pyridine, and 1,3-cyclopentanedione.

The alkaloids were the unique compounds during the thermal decomposition of tobacco materials [10], and they were proved to be the main products in the trapped particulate matters here. The effect of heating rate and

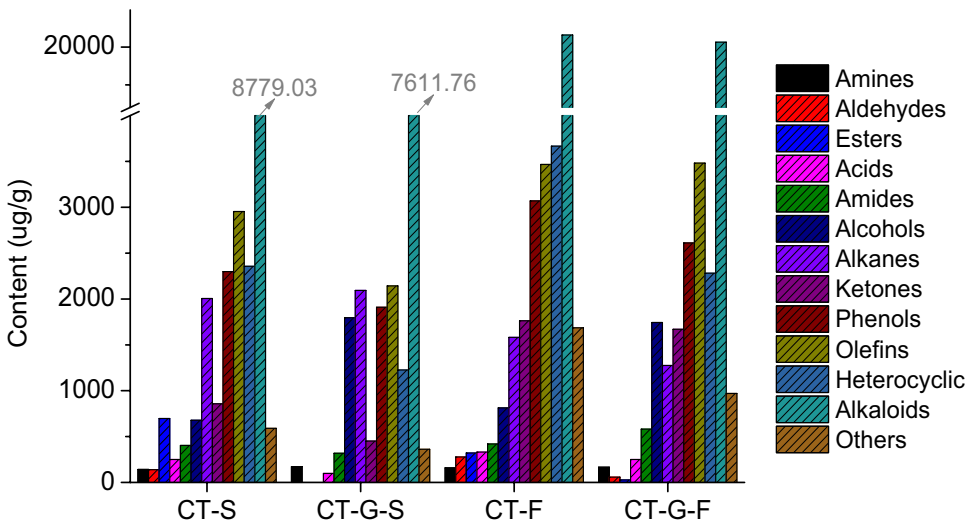

Fig. 10 The contents of different classifications of trapped pyrolytic products as for the CT and CT-G samples

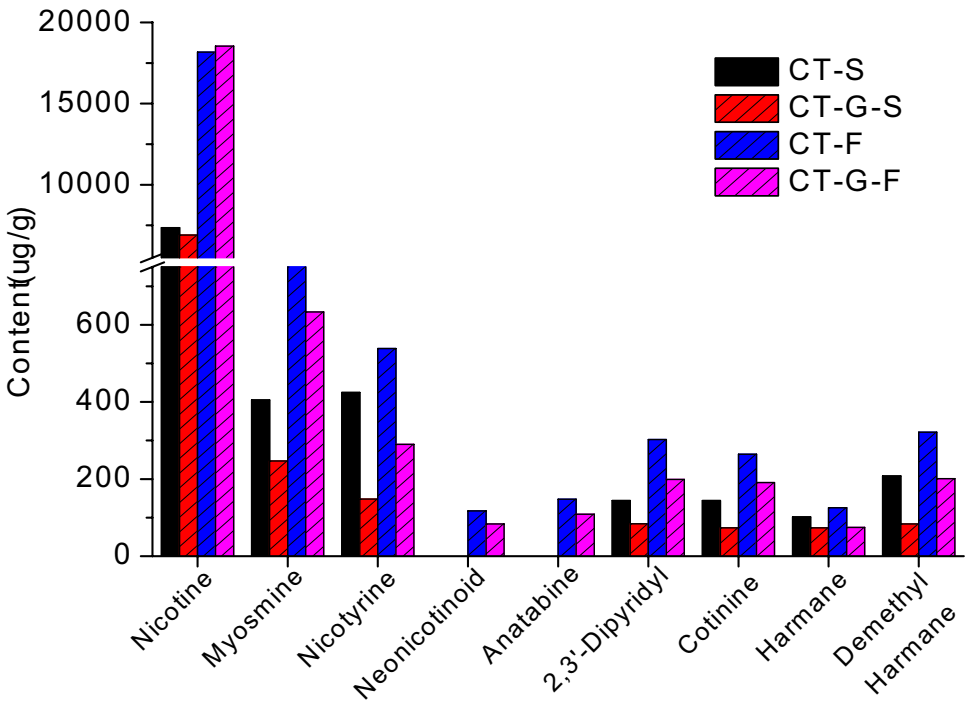

Fig. 11 The contents of different alkaloid compounds in the pyrolysis of CT and CT-G samples

glycerol on the release of various alkaloids was investigated, and the results were shown in Fig. 11. Higher heating rate resulted in an increase in the yield of all the alkaloid compounds, especially for the nicotine whose content was increased by 1.5 times. The contents of myosmine and nicotyrine were also greatly increased to 805.50 μg/g and 538.59 μg/g, respectively, as for the CT-F sample, and to 633.35 μg/g and 289.94 μg/g as for the CT-G-F sample. Neonicotinoid and anatabine were only generated under the high heating rate. In addition, the addition of glycerol inhibited the release of various alkaloids significantly, except for the nicotine, under the two selected heating rates. It should be noted that alkaloids only generated from the decomposition of tobacco itself; the content of alkaloids compounds should be increased when the mass of glycerol was deducted from the sample. These results indicated glycerol may participate in the pyrolysis process of CT and affect the distribution of pyrolytic products, which may provide basis reference for the formulation design of cigarette product.

4 Conclusions

In summary, the influence of glycerol addition on the pyrolysis characteristic, kinetic behavior, and release of pyrolytic products was investigated in this study. The whole thermal weight loss process of CT can be divided into four stages, and the addition of glycerol shifted the temperature interval of stage II to the lower temperature and increased the DTG_{max} and weight loss at this stage. T_i, T_f, and residues were decreased, while the CPI was increased as for the CT-G sample, which indicated an increased reactivity and comprehensive pyrolysis performance. Gauss peak fitting method can be well used to separate the pyrolysis of pseudocomponents in the tobacco biomass. Pyrolysis kinetic behavior of each fitted peak indicated that glycerol addition reduced the Ei for the decomposition of tobacco components. Thermodynamic parameters also indicated the improved reaction reactivity of CT-G. The effect of glycerol on the change of composition and pyrolysis property of CT was also reflected in the gaseous release behavior of CO_2, CO, aldehydes, ketones, acids, and phenols through TG-FTIR analysis. TG-MS analysis of characteristic mass fragments also indicated the glycerol addition decreased the release amount of pyrolytic products of unit mass samples. The pyrolytic products in particulate matter were trapped by Cambridge filter and analyzed by GC–MS. High heating rate was favorable for the sufficient release of pyrolytic products and aroma compounds. The glycerol slightly inhibited the generation of alkaloids, phenols, esters, ketones, acids, and heterocyclic compounds, indicating the interaction between CT and glycerol.

Supplementary Information The online version contains supplementary material available at https://doi.org/10.1007/s13399-022-03175-9.

Author contribution All authors contributed to the study conception and design. The summary is as follows. Conceptualization: Junsong Zhang and Miao Liang. Material preparation: Weiqiang Xiao and Qian Xia. Methodology: Jiabao Zhang and Jian Wu. Formal analysis and investigation: Jian Wu, Zhen Chen, Miao Liang, and Jun Wang. Writing—original draft preparation: Jian Wu and Miao Liang. Writing—review and editing: Guojun Zhou, Yiqun Wang, Jian Jiang, and Miao Liang. Funding acquisition: Guojun Zhou and Junsong Zhang. Supervision: Miao Liang and Junsong Zhang. All authors commented on previous versions of the manuscript. All authors read and approved the final manuscript.

Funding This work was supported by the Research Foundation (ZJZY2021A005) of China Tobacco Zhejiang Industrial Co., Ltd.

Data availability The datasets generated during and/or analyzed during the current study are available from the corresponding author on reasonable request.

Declarations

Conflict of interest The authors declare no competing interests.

References

1. Strezov V, Popovic E, Filkoski RV, Shah P, Evans T (2012) Assessment of the thermal processing behavior of tobacco waste. Energy Fuels 26:5930–5935
2. Wu W, Mei Y, Zhang L, Liu R, Cai J (2015) Kinetics and reaction chemistry of pyrolysis and combustion of tobacco waste. Fuel 156:71–80
3. Dai Y, Xu J, Zhu L, Jiang J, Zhou Y, Zhou G (2021) Mechanism study on the effect of glycerol addition on tobacco pyrolysis. J Anal Appl Pyrol 157:105183
4. Cong K, Han F, Zhang Y, Li Q (2019) The investigation of co-combustion characteristics of tobacco stalk and low rank coal using a macro-TGA. Fuel 237:126–132
5. Cai J, Li B, Chen C, Wang J, Zhao M, Zhang K (2016) Hydrothermal carbonization of tobacco stalk for fuel application. Biores Technol 220:305–311
6. Liang M, Zhang K, Lei P, Wang B, Shu C-M, Li B (2020) Fuel properties and combustion kinetics of hydrochar derived from co-hydrothermal carbonization of tobacco residues and graphene oxide. Biomass Convers Biorefinery 10:189–201
7. Mu Y, Peng Y, Tang X, Ren J, Xing J, Luo K, Fan J, Zhang K (2022) Experimental and kinetic studies on tobacco pyrolysis under a wide range of heating rates. ACS Omega 7:1420–1427
8. Liang M, Yang T, Zhang G, Zhang K, Wang L, Li R, He Y, Wang J, Zhang J (2021) Effects of hydrochloric acid washing on the structure and pyrolysis characteristics of tobacco stalk. Biomass Convers Biorefinery. https://doi.org/10.1007/s13399-021-01616-5
9. Chen Z, Leng E, Zhang Y, Zheng A, Peng Y, Gong X, Huang Y, Qiao Y (2018) Pyrolysis characteristics of tobacco stem after different solvent leaching treatments. J Anal Appl Pyrol 130:350–357
10. Cardoso CR, Ataíde CH (2013) Analytical pyrolysis of tobacco residue: effect of temperature and inorganic additives. J Anal Appl Pyrol 99:49–57
11. Gao W, Chen K, Xiang Z, Yang F, Zeng J, Li J, Yang R, Rao G, Tao H (2013) Kinetic study on pyrolysis of tobacco residues from the cigarette industry. Ind Crops Prod 44:152–157
12. Sung YJ, Seo YB (2009) Thermogravimetric study on stem biomass of Nicotiana tabacum. Thermochim Acta 486:1–4
13. Liu B, Li Y-M, Wu S-B, Li Y-H, Deng S-S, Xia Z-L (2012) Pyrolysis characteristic of tobacco stem studied by Py-GC/MS, TG-FTIR, and TG-MS. BioResources 8:11
14. Ye X-n, Lu Q, Li W-t, Gao P, Hu B, Zhang Z-b, Dong C-q (2016) Selective production of nicotyrine from catalytic fast pyrolysis of tobacco biomass with Pd/C catalyst. J Anal Appl Pyrol 117:88–93
15. Chen R, Zhang J, Lun L, Li Q, Zhang Y (2019) Comparative study on synergistic effects in co-pyrolysis of tobacco stalk with polymer wastes: thermal behavior, gas formation, and kinetics. Biores Technol 292:121970
16. Liu F, Wu Z, Zhang X, Xi G, Zhao Z, Lai M, Zhao M (2021) Microbial community and metabolic function analysis of cigar tobacco leaves during fermentation. MicrobiologyOpen 10:e1171
17. Chen J, He X, Zhang X, Chen Y, Zhao L, Su J, Qu S, Ji X, Wang T, Li Z, He C, Zeng E, Jin Y, Lin Z, Zou C (2021) The applicability of different tobacco types to heated tobacco products. Ind Crops Prod 168:113579
18. Carmines EL, Gaworski CL (2005) Toxicological evaluation of glycerin as a cigarette ingredient. Food Chem Toxicol 43:1521–1539
19. Gómez-Siurana A, Marcilla A, Beltrán M, Berenguer D, Martínez-Castellanos I, Menargues S (2013) TGA/FTIR study of tobacco and glycerol–tobacco mixtures. Thermochim Acta 573:146–157
20. Fan Y, Li L, Tippayawong N, Xia S, Cao F, Yang X, Zheng A, Zhao Z, Li H (2019) Quantitative structure-reactivity relationships for pyrolysis and gasification of torrefied xylan. Energy 188:116119
21. Wang T, Chen Y, Li J, Xue Y, Liu J, Mei M, Hou H, Chen S (2020) Co-pyrolysis behavior of sewage sludge and rice husk by TG-MS and residue analysis. J Clean Prod 250:119557
22. Várhegyi G, Bobály B, Jakab E, Chen H (2011) Thermogravimetric study of biomass pyrolysis kinetics. A Distributed Activation Energy Model with Prediction Tests. Energy Fuels 25:24–32
23. Soh M, Chew JJ, Liu S, Sunarso J (2019) Comprehensive kinetic study on the pyrolysis and combustion behaviours of five oil palm biomass by thermogravimetric-mass spectrometry (TG-MS) analyses. BioEnergy Res 12:370–387
24. Jiang H, Wang J, Wu S, Wang B, Wang Z (2010) Pyrolysis kinetics of phenol–formaldehyde resin by non-isothermal thermogravimetry. Carbon 48:352–358
25. Liu Y, Xin Y, Liu H, He T, Cao H, Yuan Q (2018) Comparison study of pyrolysis kinetic characteristics of cattle manure and its semi-char. Acta Energiae Solaris Sin 39:1688–1695
26. Xu Y, Chen B (2013) Investigation of thermodynamic parameters in the pyrolysis conversion of biomass and manure to biochars using thermogravimetric analysis. Biores Technol 146:485–493
27. Yang H, Yan R, Chen H, Zheng C, Lee DH, Liang DT (2006) In-depth investigation of biomass pyrolysis based on three major components: hemicellulose, cellulose and lignin. Energy Fuels 20:388–393
28. Oja V, Hajaligol MR, Waymack BE (2006) The vaporization of semi-volatile compounds during tobacco pyrolysis. J Anal Appl Pyrol 76:117–123
29. Sun J, Dutta T, Parthasarathi R, Kim KH, Tolic N, Chu RK, Isern NG, Cort JR, Simmons BA, Singh S (2016) Rapid room temperature solubilization and depolymerization of polymeric lignin at high loadings. Green Chem 18:6012–6020
30. Wang T, Rong H, Chen S, Zhou Y, Li J, Xiao Y, Xue Y (2021) TG-MS study on in-situ sulfur retention during the co-combustion of reclaimed asphalt binder and wood sawdust. J Hazard Mater 403:123911
31. Cardoso CR, Miranda MR, Santos KG, Ataíde CH (2011) Determination of kinetic parameters and analytical pyrolysis of tobacco waste and sorghum bagasse. J Anal Appl Pyrol 92:392–400

32. Zhou H, Long Y, Meng A, Chen S, Li Q, Zhang Y (2015) A novel method for kinetics analysis of pyrolysis of hemicellulose, cellulose, and lignin in TGA and macro-TGA. RSC Adv 5:26509–26516
33. Chen D, Gao D, Capareda SC, Shuang E, Jia F, Wang Y (2020) Influences of hydrochloric acid washing on the thermal decomposition behavior and thermodynamic parameters of sweet sorghum stalk. Renew Energy 148:1244–1255
34. Ma Z, Chen D, Gu J, Bao B, Zhang Q (2015) Determination of pyrolysis characteristics and kinetics of palm kernel shell using TGA–FTIR and model-free integral methods. Energy Convers Manage 89:251–259
35. Mahmood MA, Ceylan S (2021) Insights into reaction modeling and product characterization of hazelnut shell pyrolysis. BioEnergy Res. https://doi.org/10.1007/s12155-021-10341-w
36. Kruse J, Eckhardt K-U, Regier T, Leinweber P (2011) TG–FTIR, LC/MS, XANES and Py-FIMS to disclose the thermal decomposition pathways and aromatic N formation during dipeptide pyrolysis in a soil matrix. J Anal Appl Pyrol 90:164–173
37. Sangaré D, Bostyn S, Moscosa Santillán M, García-Alamilla P, Belandria V, Gökalp I (2022) Comparative pyrolysis studies of lignocellulosic biomasses: online gas quantification, kinetics triplets, and thermodynamic parameters of the process. Biores Technol 346:126598
38. Peng Y, Hao X, Qi Q, Tang X, Mu Y, Zhang L, Liao F, Li H, Shen Y, Du F, Luo K, Wang H (2021) The effect of oxygen on in-situ evolution of chemical structures during the autothermal process of tobacco. J Anal Appl Pyrol 159:105321
39. Liao J, Li Q, Chen G, Deng X, Hu Z, Chen X, Li Y (2016) Effects of heating rate on fast pyrolysis of cut filler of cigarette. Tob Sci Technol 49:44–50
40. Malika A, Jacques N, Jaafar E-F, Fatima B, Mohammed A (2016) Pyrolysis investigation of food wastes by TG-MS-DSC technique. Biomass Convers Biorefinery 6:161–172
41. Gao H, Bai J, Wei Y, Chen W, Li L, Huang G, Li P, Chang C (2022) Effects of drying pretreatment on microwave pyrolysis characteristics of tobacco stems. Biomass Convers Biorefinery. https://doi.org/10.1007/s13399-021-02120-6